AGU PUBLICATIONS

JGR

Journal of Geophysical Research: Space Physics

RESEARCH ARTICLE
10.1002/2015JA021767

Key Points:
- Chelyabinsk meteor explosion produced gravity waves and ionospheric disturbances
- These TIDs were detected by several ionosonde stations in Europe and Russia
- Y-forking of ionogram traces is the main/primary signature of these TIDs

Correspondence to:
R. Pradipta,
rezy.pradipta@bc.edu

Citation:
Pradipta, R., C. E. Valladares, and P. H. Doherty (2015), Ionosonde observations of ionospheric disturbances due to the 15 February 2013 Chelyabinsk meteor explosion, *J. Geophys. Res. Space Physics*, *120*, 9988–9997, doi:10.1002/2015JA021767.

Received 4 AUG 2015
Accepted 26 OCT 2015
Accepted article online 29 OCT 2015
Published online 17 NOV 2015

Ionosonde observations of ionospheric disturbances due to the 15 February 2013 Chelyabinsk meteor explosion

Rezy Pradipta[1], Cesar E. Valladares[1], and Patricia H. Doherty[1]

[1] Institute for Scientific Research, Boston College, Chestnut Hill, Massachusetts, USA

Abstract We report the results of our investigations on the potential ionospheric effects caused by the 15 February 2013 Chelyabinsk meteor explosion. We used the data from a number of digisonde stations located in Europe and Russia to detect the traveling ionospheric disturbances (TIDs) likely to have been caused by the meteor explosion. We found that certain characteristic signatures of the TIDs can be identified in individual ionogram records, mostly in the form of Y-forking/splitting of the ionogram traces. Based on the arrival times of the disturbances, we have inferred the overall propagation speed of the TIDs from Chelyabinsk to be 171 $\pm$ 14 m/s.

1. Introduction

In this study, we investigated the potential ionospheric effects caused by the meteor explosion that occurred over the vicinity of Chelyabinsk, Russia (55.15°N, 61.41°E) in the early morning of 15 February 2013 at approximately 03:20 UTC. We used the archived ionogram records from the digital ionogram database managed by the University of Massachusetts Lowell Center for Atmospheric Research (UMLCAR) to look for notable characteristic signatures of traveling ionospheric disturbances (TIDs) following the meteor explosion. Based on our examination of the ionogram data from digisonde stations in Europe and Russia, we found that the suspected TID signatures started to appear over these stations 2–6 h after the meteor explosion. This time delay evidently depends on the great circle distance between Chelyabinsk and the station. Furthermore, the TIDs associated with the Chelyabinsk meteor explosion mostly (but not always) manifested themselves in the data as a distinct Y-forking of the ionogram traces. This particular characteristic signature/pattern is explained in more detail in section 2 below.

Previously, there have been several reports on the observation of ionospheric effects likely caused by this meteor explosion as well. One of these reports was based on the examination of scaled parameters from vertical radio sounding measurements (e.g., f_oF_2 and h_mF_2) combined with ionospheric tomography reconstruction at a longitude sector around Moscow [*Givishvili et al.*, 2013]. Other reports were based on the analysis of total electron content (TEC) measurements from multiple ground-based GPS receiver networks [*Gokhberg et al.*, 2013; *Yang et al.*, 2014; *Perevalova et al.*, 2015]. These investigations in general found some consistent signatures of TIDs due to the meteor explosion, with an amplitude of roughly 0.1 total electron content unit (TECU) in the GPS TEC data (note: 1TECU $\equiv 10^{16}$ el m^{-2}). However, the inferred propagation speed of the ionospheric disturbances reported in these previous studies varied considerably starting from the range of 100–200 m/s up to 300–800 m/s.

On the other hand, the global International Monitoring System infrasound sensor network operated by the Comprehensive Nuclear-Test-Ban Treaty Organization (CTBTO) had also detected the lower atmospheric infrasonic waves associated with this meteor explosion as the disturbance traveled around the globe [*LePichon et al.*, 2013]. The inferred propagation speed of the infrasound waves (0.02–0.05 Hz) detected by the CTBTO sensors was in the range of 241–277 m/s. We note here that the meteorite had a mass of 9000 t, and it entered the Earth's atmosphere with a speed of roughly 17.5 km/s before exploding at an altitude of ~30 km above the ground [see, e.g., *Schiermeier*, 2013]. The energy released by the meteor explosion was estimated to be in the order of 500 kt of TNT equivalent or approximately 2×10^{15} J [see, e.g., *LePichon et al.*, 2013; *Gokhberg et al.*, 2013].

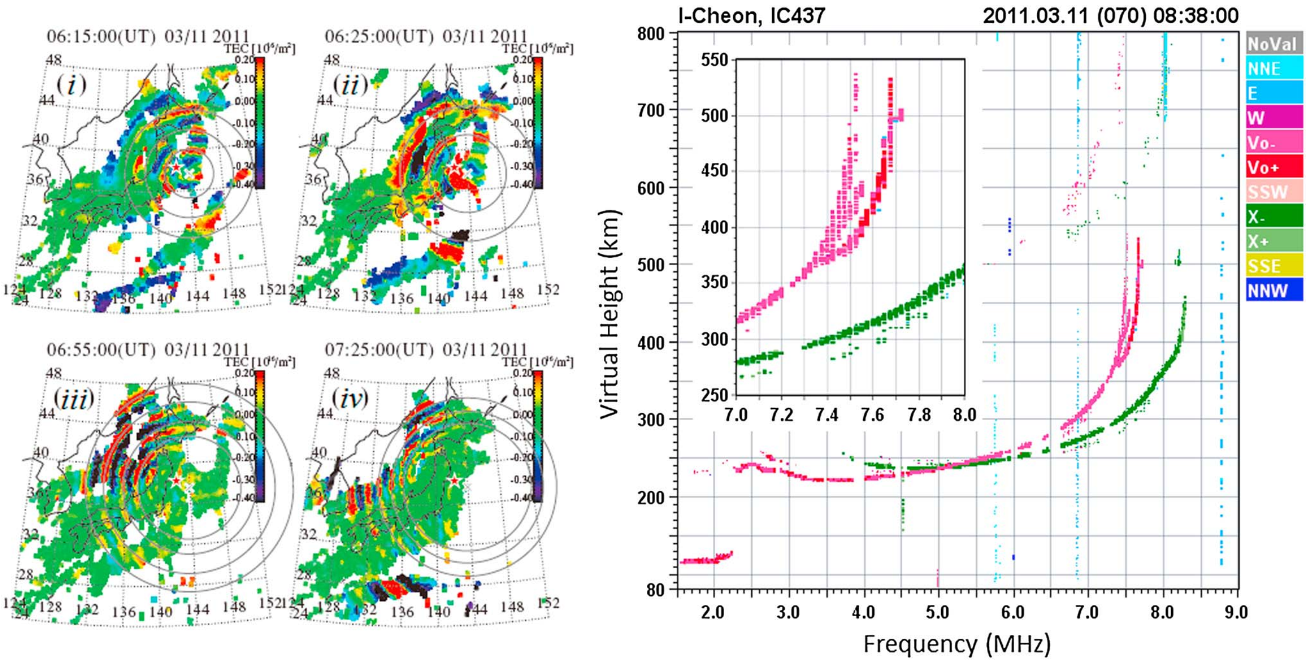

Figure 1. (left) Pattern of concentric TID wavefronts mapped using GPS TEC data recorded over Japan shortly after the 11 March 2011 Tohoku earthquake, reproduced from *Tsugawa et al.* [2011]. (right) Ionosonde data from I-Cheon, Korea, taken a few hours after the earthquake also show some characteristic signatures of these TIDs, in the form of a Y-forking of the ionogram trace.

In this paper, we identify the suspected signatures of TIDs from the Chelyabinsk meteor explosion by inspecting the individual ionosonde data records for some characteristic features/abnormalities in the observed ionogram traces (e.g., Y-forkings, splittings, or folds/bends). The arrival times of these TIDs at each station are subsequently determined based on the first/early appearance of such signatures in the ionogram traces, as opposed to looking only at the time series of scaled ionogram parameters. Based on the time delays and the great circle distances from Chelyabinsk, we have inferred the overall propagation speed to be 171 $\pm$ 14 m/s. This inferred speed very much agrees with the typical propagation speed of medium-scale TIDs (MSTIDs) from various natural and/or artificial sources [*Ogawa et al.*, 2002; *Tsugawa et al.*, 2007; *Pradipta et al.*, 2015].

The details on the setup/methodology of this study, a general survey of the ionogram observations to identify the suspected TID signatures, and the analysis/discussion of the findings are presented in the following sections below.

2. Basic Setup and Methodology

The presence of wavelike perturbations in ionospheric plasmas had been quite well known to produce certain types of characteristic signatures/abnormalities in the shape of the recorded ionogram traces [see, e.g., *Munro*, 1953; *Heisler*, 1958]. One form of such features is the Y-forking of the ionogram trace near the *F* peak penetration frequency, which was referred to as the "type A" anomaly by *Heisler* [1958]. This type of Y-forking pattern (among others) had also been obtained in numerical ray tracing studies conducted specifically to understand the effects of traveling ionospheric disturbances on high-frequency radio sounding data [*Cervera and Harris*, 2014].

Figure 1 shows a relatively more modern example of the abovementioned Y-forking pattern in ionogram records. The cluster of panels (i–iv) in Figure 1 (left) depicts a series of 2-D TECP data maps over Japan following the M_w 9.0 Tohoku earthquake on 11 March 2011. The concentric red colored circular rings around the epicenter (marked by red star) indicate the propagation of the TID wave crests over the course of several hours. Meanwhile, Figure 1 (right) shows an ionogram recorded at I-Cheon, Korea, a few hours after the earthquake. A rather distinct Y-forking of the ionogram trace can be seen here near the f_oF_2 critical frequency, with an enlarged view in the inset. The red colored traces are those of O-mode polarization, whereas the green colored traces are the X-mode polarization. Hence, note that the Y-forking happened to the O-mode trace

Figure 2. A geographic map of great circle arcs from Chelyabinsk (the meteor explosion site) toward several ionosonde stations located in Europe and Russia, using rectangular projection. The meteor explosion happened on 15 February 2013 at approximately 03:20 UTC.

itself in this case (i.e., the forking/splitting is not simply a regular distinction between the O-mode and X-mode traces). Furthermore, one might also notice that the two branches of the fork in fact have opposite doppler shifts (different shades of red, as indicated by the legend).

The above example broadly demonstrates how the characteristic signatures of TIDs may be identified in individual ionogram records, as cross checked by the GPS TEC data. While there are other types of TID signatures that could also appear in the ionograms, the Y-forking pattern was by far the most common form of TID signatures found in the data during our investigation. Using this basic principle, we monitored and noted the times when such characteristic signatures/abnormalities appeared in the ionogram records following the meteor explosion. We subsequently determined the time delay for the disturbances to reach each ionosonde station from Chelyabinsk based on the first/early appearance of the TID signatures in the data.

Figure 2 shows the map of several ionosonde stations in Europe and Russia that were used in this study. Also, overlaid on this map are the great circle arcs between Chelyabinsk (the meteor explosion site) and each of the stations. The calculated time delays and the great circle distances could then be used to infer the overall propagation speed of the disturbances. A representative survey of the ionogram observations to identify cases of suspected TID signatures from the Chelyabinsk meteor explosion over these ionosonde stations is presented in section 3 below.

3. A Survey of Ionogram Observations

In this section we discuss several cases of characteristic TID signatures that were identified in the ionograms recorded on 15 February 2013, likely related to the Chelyabinsk meteor explosion. The ionogram data were taken from eight ionosonde stations located in Europe and Russia (cf. Figure 2), and here we present some representative ionogram samples from each station around the times when the characteristic TID signatures were first observed following the meteor explosion. Most of these characteristic signatures are in the form of Y-forking of the ionogram traces, as previously outlined in section 2. However, sometimes we also observed different forms of TID signatures in the data, which would be elaborated further in our discussion below.

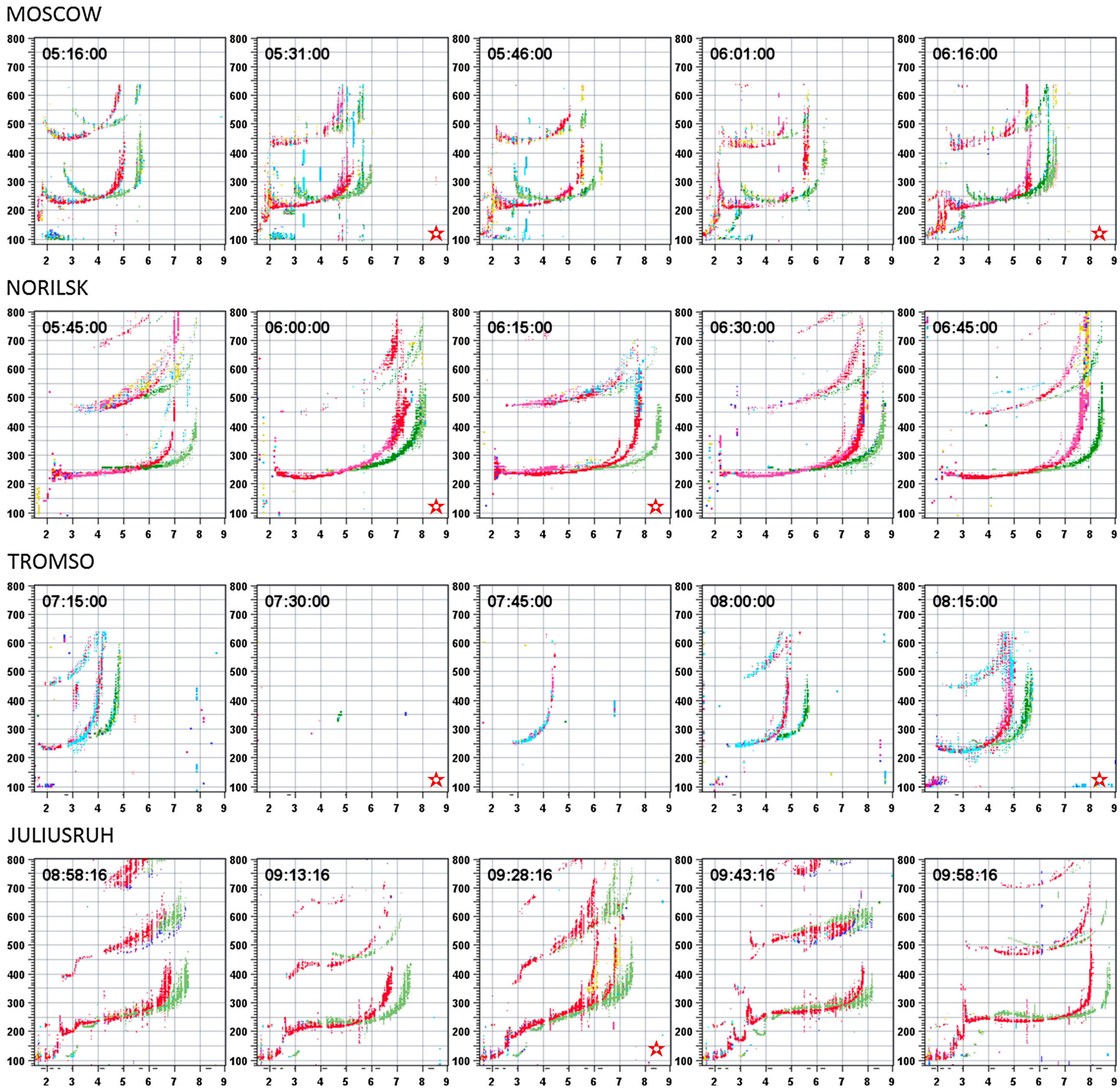

Figure 3. A survey of ionogram data taken on 15 February 2013 (from Moscow, Norilsk, Tromso, and Juliusruh stations) showing the early/first arrival of ionospheric disturbances over these stations following the meteor explosion. Each respective row depicts a set of sequential ionograms around the times when the suspected TID signatures were observed. The ionograms exhibiting the characteristic TID signatures are marked accordingly with a red star at the bottom right corner. In all of the above ionograms, the *x* axis is the sounding frequency (MHz), and the *y* axis is the virtual height (km). The ionogram traces in red color are those of O-mode polarization, and the traces in green color are those of X-mode polarization. Note that the meteor explosion itself occurred on 15 February 2013 at approximately 03:20 UTC.

Figures 3 and 4 depict several sets of sample ionograms from the eight aforementioned ionsonde stations in Europe and Russia to highlight the first/early arrival of the suspected TID signatures over these stations. Each row consists of five sequential ionograms from each station, and we have sorted the stations according to their great circle distances from Chelyabinsk (the meteor explosion site). The great circle distances were calculated based on the World Geodetic System 84 reference coordinate system using Vincenty's formula [*Vincenty*, 1975, 1976]. A number of computational tools are available online, e.g., at http://www.gcmap.com and http://www.ngs.noaa.gov/TOOLS to carry out this calculation. The one closest to Chelyabinsk is the Moscow station (1524 km), and the farthest one is the Fairford station (4056 km). Figure 3 shows the sample

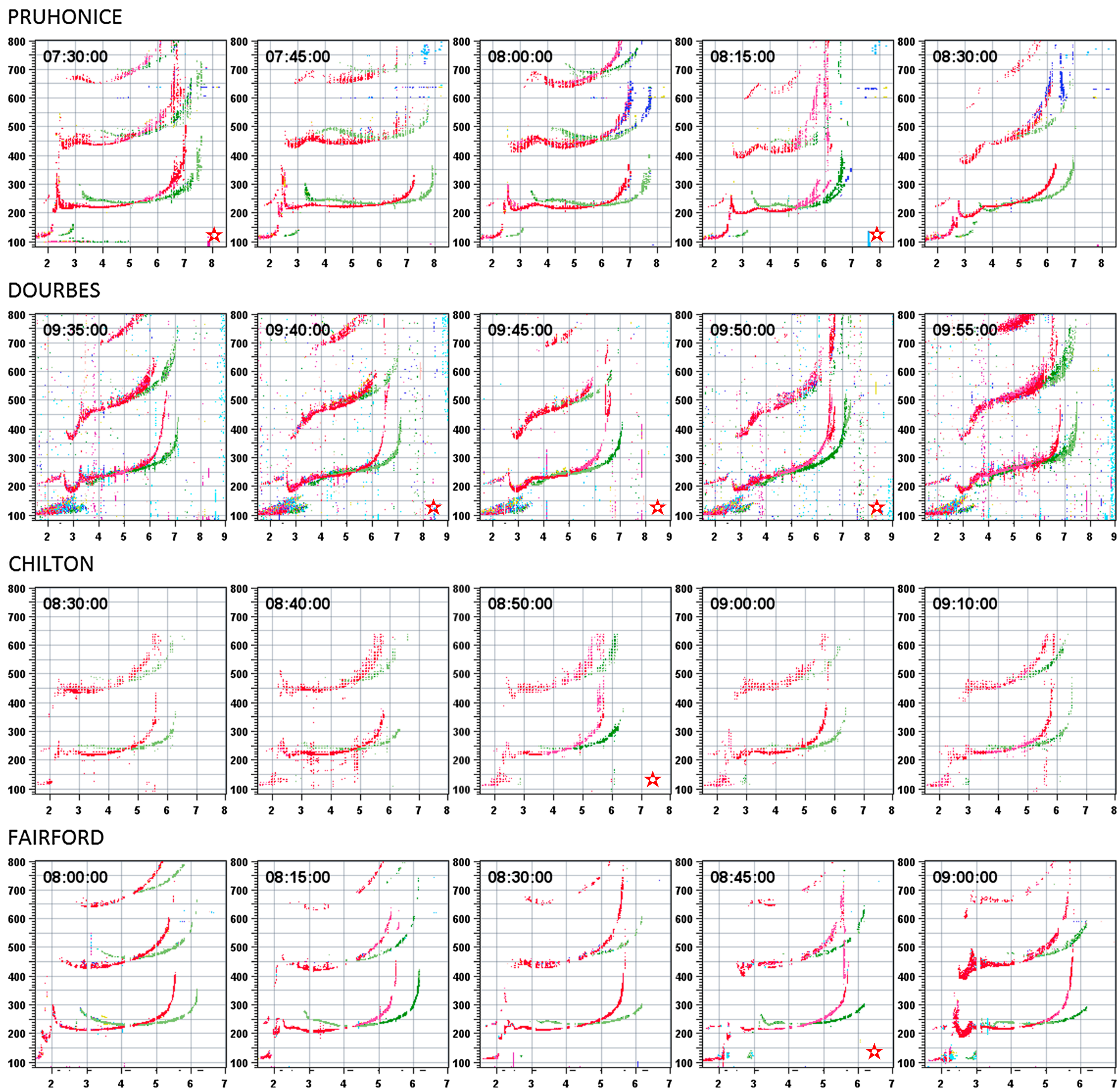

Figure 4. A survey of ionogram data taken on 15 February 2013 (from Pruhonice, Dourbes, Chilton, and Fairford stations) showing the early/first arrival of ionospheric disturbances over these stations following the meteor explosion. Each respective row depicts a set of sequential ionograms around the times when the suspected TID signatures were observed. The ionograms exhibiting the characteristic TID signatures are marked accordingly with a red star at the bottom right corner. In all of the above ionograms, the *x* axis is the sounding frequency (MHz), and the *y* axis is the virtual height (km). The ionogram traces in red color are those of O-mode polarization, and the traces in green color are those of X-mode polarization. Note that the meteor explosion itself occurred on 15 February 2013 at approximately 03:20 UTC.

ionogram records from Moscow, Norilsk, Tromso, and Juliusruh stations. Meanwhile, Figure 4 shows the sample ionogram records from Pruhonice, Dourbes, Chilton, and Fairford stations. The specific ionograms that contain the characteristic TID signatures are marked accordingly with a red star sign.

In the Moscow station data, a Y-forking of the ionogram traces was first observed at 05:31 UTC (Figure 3, first row). As a comparison, the ionogram records just before (05:16 UTC) and after (05:46 UTC) did not show any such Y-forking. The Y-forking pattern in this case could be seen in both O-mode and X-mode traces. The forking is evidently more distinct on the X-mode trace, with the two branches of the fork showing opposite doppler shift (darker and lighter shades of green). Furthermore, at 06:16 UTC one may also recognize a splitting

Table 1. A List of Several Ionosonde Stations in Europe/Russia, Their Geographic Coordinates and Great Circle Distances From Chelyabisnk, and the Earliest Time(s) When Suspected TID Signatures From the Meteor Explosion Were Observed in the Ionogram Records[a]

Ionosonde Station	Coordinate	Distance	$t_{DETECTION}$	Δt	General Remarks
Moscow (MO155)	55.47°N, 37.3°E	1524 km	05:31 UTC	2.18 h	Y-forking
			06:16 UTC	2.93 h	split trace
Norilsk (NO369)	69.2°N, 88°E	2057 km	06:00 UTC	2.67 h	Y-forking
			06:15 UTC	2.92 h	Z-mode trace/forking
Tromso (TR169)	69.6°N, 19.2°E	2627 km	07:30 UTC	4.17 h	traces disappeared
			08:45 UTC	5.42 h	slight Y-forking, spread echoes
Juliusruh (JR055)	54.6°N, 13.4°E	3021 km	09:28 UTC	6.13 h	Z-mode trace/forking
Pruhonice (PQ052)	50°N, 14.6°E	3163 km	07:30 UTC	4.17 h	Y-forking
			08:15 UTC	4.92 h	Y-forking
Dourbes (DB049)	50.1°N, 4.6°E	3779 km	09:25 UTC	6.08 h	Y-forking
			09:40 UTC	6.33 h	Y-forking
			09:45 UTC	6.42 h	Y-forking
			09:50 UTC	6.50 h	Y-forking
Chilton (RL052)	51.5°N, 0.6°W	4014 km	08:50 UTC	5.50 h	slight forking/split
Fairford (FF051)	51.7°N, 1.5°W	4056 km	08:45 UTC	5.42 h	slight forking/split

[a]The meteor explosion happened over the vicinity of Chelyabinsk (55.15°N, 61.41°E) on 15 February 2013 at approximately 03:20 UTC.

of the ionogram traces: at a sounding frequency of ~2 MHz for the O-mode trace (virtual height between 100 and 200 km) and at a sounding frequency of ~6.5 MHz for the X-mode trace (virtual height between 250 and 450 km). For the X-mode trace, once again we see that the two branches of the split/fork show opposite doppler shift.

In the Norilsk station data, the first Y-forking of the ionogram traces can be seen at 06:00 UTC (Figure 3, second row). In this ionogram record, part of the O-mode trace (around the f_oF_2 frequency of ~7 MHz) branched out from the standard vertical alignment. In the next ionogram record (06:15 UTC), we can also see another forking pattern near the f_oF_2 penetration frequency. In this case, one branch of the O-mode trace formed a vertical asymptote at ~7 MHz, while the other did so at ~7.7 MHz. The trace with the 7 MHz asymptote could still be seen in the two subsequent ionograms (06:30 and 06:45 UTC), although its intensity had faded significantly. Similar features were also observed at the Juliusruh station data, as discussed later below.

In the Tromso station data, we observed that the ionogram traces had disappeared at 07:30 UTC and recovered gradually after 30 min or so (Figure 3, third row). Over the course of this time period (07:15–08:00 UTC), we note that the f_oF_2 had actually changed from 4 MHz to 5 MHz. Finally, the ionogram at 08:15 UTC showed some frequency spreading with a hint of slight forking (on the X-mode trace).

In the Juliusruh station data, we can see that the ionogram at 09:28 UTC had two well-separated O-mode traces (Figure 3, fourth row). One formed a vertical asymptote at ~6 MHz and the other at ~7 MHz. Based on the depicted ionogram sequence, we might deduce that the f_oF_2 at this time was actually around 7 MHz. The reason for the additional trace with the 6 MHz asymptote in this case probably involves a Z-mode tunneling at the Spitze angle [e.g., *Piggott and Rawer*, 1972; *Giraud and Petit*, 1978; *Budden*, 1988], facilitated by some wavelike disturbances in the ionospheric plasma layer.

In the Pruhonice station data, notable Y-forking of the ionogram traces was first observed at 07:30 UTC and later at 08:15 UTC (Figure 4, first row). The forking that occurred at 07:30 UTC was a bit blurry and only visible on the O-mode trace. On the other hand, the forking at 08:15 UTC is more clearly visible on both O-mode and X-mode traces.

In the Dourbes station data, several cases of Y-forkings can be seen in the depicted ionogram sequence (Figure 4, second row). The first case (09:40 UTC) only shows a slight forking, but the one afterward (09:45 UTC) shows a more distinct forking of the O-mode trace. Finally, the ionogram at 09:50 UTC shows a clearly visible Y-forking on the O-mode as well as the X-mode traces.

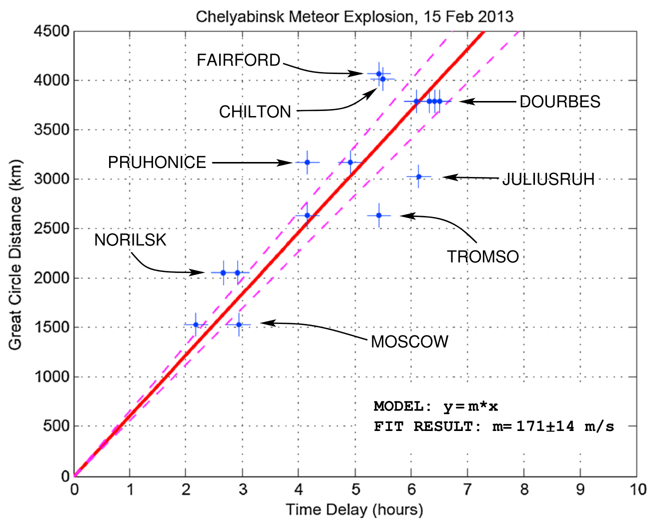

Figure 5. A plot of the great circle distance from Chelyabinsk to each ionosonde stations versus the corresponding time delay for the traveling ionospheric disturbances to arrive. The result of a linear fit to the data points is also overlaid on the graph (solid red line), revealing a propagation speed of roughly 171 m/s. The dashed magenta lines indicate the 95% confidence interval bounds.

In the Chilton station data, an unusual type of forking on the ionogram traces was observed at 08:50 UTC (Figure 4, third row). In this case, the characteristic signature can be seen only on the O-mode trace. It appeared somewhat like a frequency spreading, although it was on the "wrong" side of the ionogram trace. Here it seemed that a part of the O-mode trace (near f_oF_2) was bent leftward from the standard vertical alignment, giving rise to the observed features. In the discussion by *Heisler* [1958], this type of features (associated with the passage of TIDs) was referred to as the "type D" or "cusp" anomaly.

In the Fairford station data, similar features were also observed at 08:45 UTC (Figure 4, fourth row). Similar to what we observed at Chilton, part of the O-mode trace in this ionogram (near f_oF_2) was bent leftward from the standard vertical alignment and gave rise to this type of features.

An overall summary of this ionogram data survey is shown in Table 1. In the following section below, we present some further analysis and discussion of our findings.

4. Data Discussion

Figure 5 shows a graph where we plotted the great circle distances of each ionosonde stations from Chelyabinsk versus the corresponding time delays for the TIDs to arrive (cf. Table 1). Here the time delay is $\Delta t = t_{\mathrm{DETECTION}} - t_0$, where $t_0 \equiv$ 03:20 UTC on 15 February 2013. The individual station names are also indicated on the graph. The size of the blue crosses roughly indicates the worst-case error in Δt, based on the slowest sounder cadence in this ionosonde network (i.e., one ionogram every 15 min). The solid red line shows the result of a linear fit to the data (forcing a zero intercept at the origin), and the dashed magenta lines indicate the 95% confidence interval bounds of the fit. The slope of the fit line would correspond to the propagation speed of the ionospheric disturbances, which had been inferred to be 171 ± 14 m/s.

The sounder cadence introduces some error in the onset time $t_{\mathrm{DETECTION}}$ for each ionosonde station, but it does not contribute any error in the reference time of meteor explosion t_0. In fact, t_0 is already known to a very high precision based on orbital calculations and multiple video camera recordings [see, e.g., *Borovicka et al.*, 2013]. The sounder cadence would undoubtedly contribute some uncertainties in the time delay Δt, but this error is much smaller than the actual spread of the data points. Overall, we determined that the uncertainties due to sounder cadence have negligible effects on the fit.

This propagation speed (~171 m/s) is notably lower than that of the infrasonic waves detected by the CTBTO sensors (~260 m/s). This discrepancy is understandable since these two types of disturbances were present in separate altitude range: the CTBTO sensors measured disturbances in the lower troposphere, whereas our ionosonde measurements are concerned about disturbances that propagated in the

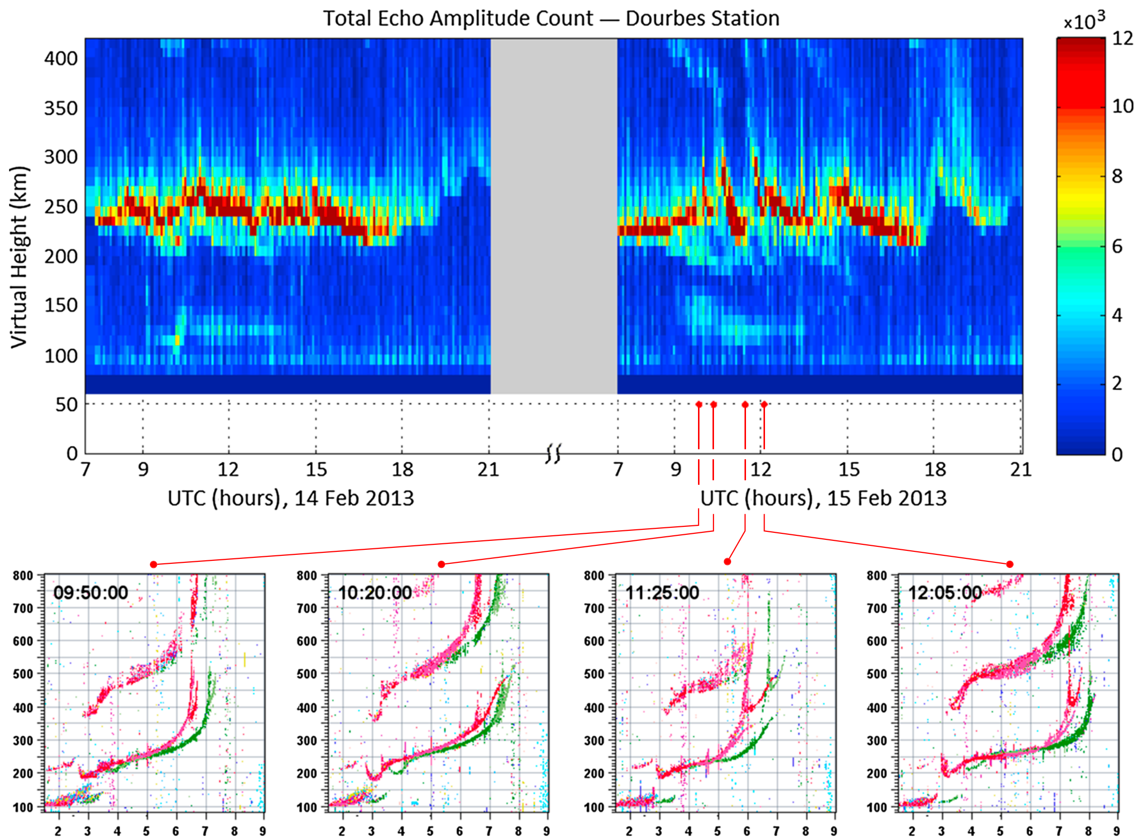

Figure 6. An RTI-style plot of ionogram data from the Dourbes station, covering a representative time window 07:00–21:00 UTC on 14 and 15 February 2013. The colormap indicates the level of the total echo amplitude count at any given virtual height and time, summed over all sounding frequencies. Shown also are samples of individual ionogram at four specific times during the passage of ionospheric disturbances over this station after the Chelyabinsk meteor explosion several hours earlier. See text for a more detailed discussion.

thermosphere/ionosphere. Atmospheric shockwaves/disturbances in the lower troposphere in general would propagate nondispersively at the adiabatic sound speed $c_s = \sqrt{\gamma k_B T/M}$ [see, e.g., *Landau and Lifshitz*, 1987; *Wong*, 1986], which is in the order of 300 m/s. On the other hand, similar disturbances at ionospheric altitudes would propagate at a speed dictated mostly by the dispersion relation for acoustic-gravity waves, which has a rather wide range of values in the order of several hundreds of m/s [see, e.g., *Hines*, 1960]. It is also generally accepted that large-scale TIDs propagate at a significantly higher velocity (and survive a longer propagation distance) than smaller-scale TIDs [see, e.g., *Francis*, 1973]. For the most part, the speed inferred in this analysis (~171 m/s) is closer to the typical propagation speed of medium-scale TIDs (MSTIDs) from natural as well as artificial sources [*Ogawa et al.*, 2002; *Tsugawa et al.*, 2007; *Pradipta et al.*, 2015].

Figure 6 depicts a plot of the total ionogram echo count (from the Dourbes station) as a function of virtual height and time—i.e., a kind of range-time-intensity plot. The level of the total echo amplitude count (i.e., the total sum of the dBm amplitudes, integrated over all sounding frequencies) at any given virtual height and time is indicated by the colormap. Note that the total echo amplitude count is not equal to the integrated power in dBW but more of a relative measure for the total number of digitized echoes (dBm amplitude weighted). This RTI-style plot covers a representative time window of 07:00–21:00 UTC on two consecutive days (14 and 15 February 2013). On 14 February 2013 (one day before the meteor explosion), the ionospheric plasma layer during this time period appeared to be rather calm without any drastic vertical displacements. There were some wavelike variations that can be discerned, but their magnitudes were only ~20 km or less in terms of vertical displacement. Meanwhile, the ionospheric plasma layer on 15 February 2013 (the day of the Chelyabinsk meteor explosion) during this time period showed a series of large (> 50 km) vertical displacements. These sharp rises and subsequent descents of the ionospheric reflection height undoubtedly indicate the passage of TIDs over this ionosonde station, following the Chelyabinsk meteor explosion that occurred a few hours earlier on that day.

Several samples of individual ionogram at four selected times are also shown in Figure 6 (bottom). These ionograms were recorded during the passage of the TIDs that we identified above (likely to have come from the meteor explosion), and we can clearly see the distinct Y-forking pattern of the ionogram traces in all of them. The Y-forkings are much more pronounced on the O-mode traces, but they are visible on the X-mode traces as well.

Finally, we note here that the Chelyabinsk meteor explosion (a natural event) shared a remarkably similar geometry with some high-altitude nuclear detonations, which had also been known to produce significant level of ionospheric disturbances [e.g., *Obayashi*, 1963; *Wickersham*, 1966; *Hines*, 1967]. In such cases, the substantial vertical separation between the ground and the explosion point would in general make the shock wave reflection pattern considerably more complex than that of a simple ground explosion. Hence, the wave disturbance might enter the thermosphere/ionosphere at various incidence angles in more than one single stage, potentially creating a wider range of characteristic features for the induced TIDs. In the case of high-altitude nuclear detonations, the typical TID propagation speed that had been previously reported ranges from 50 to 900 m/s [*Obayashi*, 1962; *Breitling et al.*, 1967]. These ranges of values were further corroborated by the theoretical velocity distribution curves for ducted acoustic-gravity waves in the ionosphere [*Wickersham*, 1965]. Comparatively, the TID propagation speed inferred in our analysis (~171 m/s; from the Chelyabinsk meteor explosion) is also in agreement with the dominant modes described in the abovementioned theoretical distribution.

5. Conclusions

We have presented the results of our ionosonde data analysis to identify the suspected ionospheric disturbances likely caused by the meteor explosion over Chelyabinsk on 15 February 2013. More specifically, in this study we monitored the individual ionogram records to look for certain kind of characteristic patterns—mostly in the form of Y-forking of the ionogram traces. Such Y-forking patterns would in general indicate the presence of TIDs over the ionosonde station, as we briefly demonstrated (in section 2) using the 11 March 2011 Tohoku earthquake as a case study. We had used this scheme to determine the arrival time of the ionospheric disturbances caused by the meteor explosion, which might not be so obvious from the time series of scaled ionogram parameters (e.g., h_mF_2, f_oF_2, and N_mF_2) alone.

Using the data from eight ionosonde stations located in Europe and Russia, we subsequently inferred the propagation speed of the ionospheric disturbances associated with the Chelyabinsk meteor explosion to be 171 $\pm$ 14 m/s. The propagation speed was calculated based on the great circle distance from Chelyabinsk and the time delay since the meteor explosion (03:20 UTC on 15 February 2013) until the first/early arrival of the disturbances over each respective ionosonde stations. The inferred speed (~171 m/s) falls in the range of the typical propagation speed for MSTIDs [e.g., *Ogawa et al.*, 2002; *Tsugawa et al.*, 2007], and it is also in general agreement with the speed of anomalous TIDs associated with high-altitude detonations that had been observed and analyzed in the past [e.g., *Obayashi*, 1963; *Wickersham*, 1965; *Hines*, 1967].

In summary, a set of anomalous ionospheric plasma disturbances likely caused by the Chelyabinsk meteor explosion on 15 February 2013 were detectable by a number of ionosonde stations in Europe and Russia. We demonstrated here that the characteristic signatures of these TIDs can be recognized predominantly as a distinct Y-forking of the ionogram traces. By identifying these characteristic signatures in individual ionogram records, we were able to determine the precise arrival times of the disturbances and infer the corresponding propagation speed. These precise arrival times might not necessarily be clear-cut enough if they were based on the time series of scaled ionogram parameters alone. It is thus important that the aforementioned unique characteristic patterns (such as the Y-forking) in individual ionograms be utilized to the optimal extent.

Acknowledgments
This work was supported by FAA grant FAA,11-G-006 at Boston College. One of the authors, Valladares, was partially supported by Air Force Research Laboratory contract FA8718-09-C-0041, NSF grants ATM-1135675 and ATM-1242476, and NASA LWS grant NNX11AP02G. We also thank the University of Massachusetts Lowell Center for Atmospheric Research (UMLCAR) for the ionogram data provided at http://ulcar.uml.edu/DIDBase/.

References

Borovicka, J., P. Spurny, P. Brown, P. Wiegert, P. Kalenda, D. Clark, and L. Shrbeny (2013), The trajectory, structure and origin of the Chelyabinsk asteroidal impactor, *Nature*, *503*, 235–237, doi:10.1038/nature12671.

Breitling, W. J., R. A. Kupferman, and G. J. Gassmann (1967), Traveling ionospheric disturbances associated with nuclear detonations, *J. Geophys. Res.*, *72*(1), 307–315, doi:10.1029/JZ072i001p00307.

Budden, K. G. (1988), *The Propagation of Radio Waves: The Theory of Radio Waves of Low Power in the Ionosphere and Magnetosphere*, Cambridge Univ. Press, Cambridge, New York.

Cervera, M. A., and T. J. Harris (2014), Modeling ionospheric disturbance features in quasi-vertically incident ionograms using 3-D magnetoionic ray tracing and atmospheric gravity waves, *J. Geophys. Res. Space Physics*, *119*, 431–440, doi:10.1002/2013JA019247.

Francis, S. H. (1973), Acoustic-gravity modes and large-scale traveling ionospheric disturbances of a realistic, dissipative atmosphere, *J. Geophys. Res.*, *78*(13), 2278–2301, doi:10.1029/JA078i013p02278.

Giraud, A., and M. Petit (1978), *Ionospheric Techniques and Phenomena*, Geophysics and Astrophysics Monographs, vol. 13, Springer, Netherlands.

Givishvili, G. V., L. N. Leshchenko, V. V. Alpatov, S. A. Grigor'eva, S. V. Zhuravlev, V. D. Kuznetsov, O. A. Kusonskii, V. B. Lapshin, and M. V. Rybakov (2013), Ionospheric effects induced by the Chelyabinsk meteor, *Sol. Syst. Res.*, *47*(4), 280–287, doi:10.1134/S0038094613040138.

Gokhberg, M. B., E. V. Ol'shanskaya, G. M. Steblov, and S. L. Shalimov (2013), The Chelyabinsk meteorite: Ionospheric response based on GPS measurements, *Dokl. Earth Sci.*, *452*(1), 948–952, doi:10.1134/S1028334X13090109.

Heisler, L. H. (1958), Anomalies in ionosonde records due to travelling ionospheric disturbances, *Aust. J. Phys.*, *11*(1), 79–90.

Hines, C. O. (1960), Internal atmospheric gravity waves at ionospheric heights, *Can. J. Phys.*, *38*(11), 1441–1481.

Hines, C. O. (1967), On the nature of traveling ionospheric disturbances launched by low-altitude nuclear explosions, *J. Geophys. Res.*, *72*(7), 1877–1882, doi:10.1029/JZ072i007p01877.

Landau, L. D., and E. M. Lifshitz (1987), *Fluid Mechanics*, 2nd ed., Course of Theoretical Physics, vol. 6, Butterworth-Heinenann, London.

LePichon, A., L. Ceranna, C. Pilger, P. Mialle, D. Brown, P. Herry, and N. Brachet (2013), The 2013 Russian fireball largest ever detected by CTBTO infrasound sensors, *Geophys. Res. Lett.*, *40*, 3732–3737, doi:10.1002/grl.50619.

Munro, G. H. (1953), Reflexions from irregularities in the ionosphere, *Proc. R. Soc. London A*, *219*, 447–463, doi:10.1098/rspa.1953.0159.

Obayashi, T. (1962), Widespread ionospheric disturbances due to nuclear explosions during October 1961, *Nature*, *196*(4849), 24–27.

Obayashi, T. (1963), Upper atmospheric disturbances due to high altitude nuclear explosions, *Planet. Space Sci.*, *10*, 47–63.

Ogawa, T., N. Balan, Y. Otsuka, K. Shiokawa, C. Ihara, T. Shimomai, and A. Saito (2002), Observations and modeling of 630 nm airglow and total electron content associated with traveling ionospheric disturbances over Shigaraki, Japan, *Earth Planets Space*, *54*, 45–56.

Perevalova, N. P., N. V. Shestakov, S. V. Voeykov, H. Takahashi, and M. Guojie (2015), Ionospheric disturbances in the vicinity of the Chelyabinsk meteoroid explosive disruption as inferred from dense GPS observations, *Geophys. Res. Lett.*, *42*, 6535–6543, doi:10.1002/2015GL064792.

Piggott, W. R., and K. Rawer (Eds.) (1972), *URSI Handbook of Ionogram Interpretation and Reduction*, 2nd ed., U. S. Department of Commerce, National Oceanic and Atmospheric Administration, Environmental Data Service, Asheville, N. C.

Pradipta, R., M. C. Lee, J. A. Cohen, and B. J. Watkins (2015), Generation of artificial acoustic-gravity waves and traveling ionospheric disturbances in HF heating experiments, *Earth Moon Planets*, *116*(1), 67–78, doi:10.1007/s11038-015-9461-2.

Schiermeier, Q. (2013), The death of the Chebarkul meteor, *Nature*, *495*, 16–17.

Tsugawa, T., Y. Otsuka, A. J. Coster, and A. Saito (2007), Medium-scale traveling ionospheric disturbances detected with dense and wide TEC maps over North America, *Geophys. Res. Lett.*, *34*, L22101, doi:10.1029/2007GL031663.

Tsugawa, T., A. Saito, Y. Otsuka, M. Nishioka, T. Maruyama, H. Kato, T. Nagatsuma, and K. T. Murata (2011), Ionospheric disturbances detected by GPS total electron content observation after the 2011 off the Pacific coast of Tohoku Earthquake, *Earth Planets Space*, *63*, 875–879.

Vincenty, T. (1975), Direct and inverse solutions on the ellipsoid with application of nested equations, *Surv. Rev.*, *23*(176), 88–93.

Vincenty, T. (1976), Correspondence: Solutions of geodesics, *Surv. Rev.*, *23*(180), 294.

Wickersham, A. F. Jr. (1965), Comparison of velocity distributions for acoustic-gravity waves and traveling ionospheric disturbances, *J. Geophys. Res.*, *70*(19), 4875–4883, doi:10.1029/JZ070i019p04875.

Wickersham, A. F. Jr. (1966), Identification of acoustic-gravity wave modes from ionospheric range-time observations, *J. Geophys. Res.*, *71*(19), 4551–4555, doi:10.1029/JZ071i019p04551.

Wong, G. S. K. (1986), Speed of sound in standard air, *J. Acoust. Soc. Am.*, *79*(5), 1359, doi:10.1121/1.393664.

Yang, Y.-M., A. Komjathy, R. B. Langley, P. Vergados, M. D. Butala, and A. J. Mannucci (2014), The 2013 Chelyabinsk meteor ionospheric impact studied using GPS measurements, *Radio Sci.*, *49*, 341–350, doi:10.1002/2013RS005344.